

¹ A Design for a Deep Underground Single-Phase
² Liquid Argon Time Projection Chamber for
³ Neutrino Physics and Astrophysics

⁴ April 1, 2015

Contents

1	Detector Development Program	1
2	1.1 Introduction	1
3	1.2 Components of the Development Program	2
4	1.3 Materials Test System	2
5	1.4 TPC Design	6
6	1.5 35-ton Prototype: Phase 1	7
7	1.5.1 Phase 1 Construction	8
8	1.5.2 Phase 1 Instrumentation	10
9	1.5.3 Phase 1 Operations	11
10	Gas Phase	11
11	Cool down and LAr filling	13
12	LAr Purification	14
13	1.5.4 Phase 1 Stability of Operation	14
14	1.5.5 Phase 1 Conclusions	18
15	1.6 35t Prototype Phase 2	18
16	1.6.1 35t Phase 2 TPC Design	18
17	1.6.2 Phase 2 Simulation, Reconstruction and Analysis	18
18	1.7 Prototype Detector at CERN to Test Physics Sensitivity	21
19	1.8 Physics Experiments with Associated Detector-Development Goals	22
20	1.8.1 ArgoNeuT - T962	22
21	1.8.2 MicroBooNE E-974	23
22	1.9 Summary	26

¹ List of Figures

²	1.1	Liquid argon area at the Proton Assembly Building at Fermilab	4
³	1.2	Schematic of the Materials Test System (MTS) cryostat at Fermilab	5
⁴	1.3	Layout of 35-ton prototype at Fermilab's PC-4 facility	9
⁵	1.4	Cutaway view	9
⁶	1.5	Gas Ar Purge and Recirculation	12
⁷	1.6	35t Cooldown and Filling	13
⁸	1.7	35t Vapor Flow	15
⁹	1.8	35t Electron Lifetime	16
¹⁰	1.9	35t Temperature Stability	17
¹¹	1.10	35t Vertical Temperature Profile	19
¹²	1.11	35t with TPC	20
¹³	1.12	ArgoNeuT neutrino event with four photon conversions	23
¹⁴	1.13	Data from ArgoNeuT	24
¹⁵	1.14	ArgoNeuT: status of 3D reconstruction	25
¹⁶	1.15	ArgoNeuT: status of calorimetric reconstruction	26

1

v

List of Tables

2	1.1	LBNE on-project development activities	3
3	1.2	LBNE off-project development activities	3
4	1.3	35t Details and Dimensions	10
5	1.4	35t Design Elements	20

¹ Todo list

² add ref?	1
³ This section needs review	2
⁴ Do we need to say how old the MTS is?	2
⁵ today's to-date is different from when this was written	4
⁶ incomplete sentence	6
⁷ right?	6
⁸ add citation	6
⁹ add citation	7
¹⁰	17
¹¹	17

¹ Chapter 1

² Detector Development Program

ch:randd

³ 1.1 Introduction

⁴ This chapter describes the development program designed to ensure a successful
⁵ and cost-effective construction and operation of the massive, dual-cryostat LArTPC
⁶ detector for LBNE and to investigate possibilities for enhancing the performance of
⁷ the detector. The feasibility of the LArTPC as a detector has been demonstrated
⁸ most impressively by the ICARUS experiment.

⁹ add ref?

¹⁰ It is understood that for successful operation an LArTPC has stringent require-
¹¹ ments on

- ¹² • argon purity, which must be of order 200 ppt O₂ equivalent or better
- ¹³ • long-term reliability of components located within the liquid argon; in partic-
¹⁴ ular, the TPC and field cage must be robust against wire-breakage and must
¹⁵ support a cool-down of over 200 K
- ¹⁶ • the front-end electronics, which must achieve a noise level ENC of 1000e or
¹⁷ better

¹⁸ The design of the LBNE LArTPC has evolved significantly from earlier concepts
¹⁹ based on standard, above-ground, upright cylindrical LNG storage tanks which envi-
²⁰ sioned single TPC sense and high-voltage planes spanning the full width of the tank
²¹ – essentially a direct scaling of previous detectors. Problems with the actual con-
²² struction of such massive planes and with the logistics of being able to construct the
²³ TPC only after the cryostat was complete are avoided in the present design. In this

1 design, TPC ‘panels’ are fully assembled and tested — including the electronics —
2 independently of the cryostat construction. This modular approach is a key feature
3 of the design. It has the benefit not only of improving the logistics of detector con-
4 struction, but also the individual components can be of manageable size. It should
5 also be noted that the cryostat itself is formed of modular panels designed for quick
6 and convenient assembly.

1.2 Components of the Development Program

:comp-dev-prog
7 This section needs review
8

9 Programs of ongoing and planned development to allow the construction of mas-
10 sive LArTPCs in the U.S. have been developed and described in the *Integrated Plan*
11 *for LArTPC Neutrino Detectors in the US* [6]. To advance the technology to the
12 detectors proposed for LBNE, the U.S. program has three aspects:

- 13 • a demonstration that the U.S program can reproduce the essential elements of
14 the existing technology of the ICARUS program
- 15 • a program of development on individual elements to improve the technology
16 and/or make it more cost-effective
- 17 • a program of development on how to apply the technology to a detector module

18 A summary of the items in the program is given in the following tables. Table 1.1
19 lists the activities that are part of the LBNE Project (“on-project”) described in this
20 chapter, a short description of the information needed and the LBNE milestone cor-
21 responding to when the information is required. Table 1.2 lists off-project activities,
22 the aspect of these activities that is applicable to LAr-FD and the LBNE milestone
23 at which the information is required. These aspects will be described in more detail
24 in the following sections. As will be explained below, these are not R&D activities,
25 but rather elements of the preliminary engineering design process.

1.3 Materials Test System

sec:mts
26 Do we need to say how old the MTS is?

27 An area for LAr detector development, shown in Figure 1.1, has been established
28 in the Proton Assembly Building at Fermilab. The Materials Test System (MTS)

fig:PAB

Table 1.1: LBNE on-project development activities

Activity	LAr-FD Information	Need by
In-liquid Electronics	Low noise readout, long lifetime	CERN prototype construction
TPC Construction	Mechanical design	CERN prototype construction
35-ton Prototype	Cryostat construction	CERN prototype cryostat procurement
CERN prototype	detector integration	TPC construction

tab:on-project

Table 1.2: LBNE off-project development activities

Activity	LAr-FD Applicability	Status	Need by
Yale TPC	None	Completed	NA
Materials System	Test	Define requirements	Completed
		Materials testing	Operating
Electronics Stand	Test	Electronics testing	Operating
LAPD	Purity w/o evac. Convective flow	Operating Operating	LBNE CD2 LBNE CD2
Scintillator Development	De-	Photon Det. Definition	Completed
		Industrialization	Not started
ArgoNeuT	Analysis tools	On-going	LBNE CD2
MicroBooNE	Electronics tests DAQ algorithms Analysis tools Lessons learned	Construction In development In development Not started	LBNE CD3 LBNE CD3 LBNE CD2 LBNE CD3

tab:off-project

1 has been developed to determine the effect on electron-drift lifetime of materials
 2 and components that are candidates for inclusion in LAr-FD. The system essentially
 3 consists of a source of clean argon (< 30 ppt O₂ equivalent), a cryostat, a sample
 4 chamber that can be purged or evacuated, a mechanism for transferring a sample
 5 from the sample chamber into the cryostat, a mechanism for setting the sample
 6 height in the cryostat so that it can be placed either in the liquid or in the gas ullage
 7 above the liquid, a temperature probe to measure the temperature of the sample,
 8 and an electron-lifetime monitor. The system is fully automated and the lifetime
 9 data are stored in a single database along with the state of the cryogenic system.



Figure 1.1: Liquid argon area at the Proton Assembly Building at Fermilab

fig:PAB

10 A noteworthy feature is the novel bubble-pump filter inside the cryostat. In case
 11 of argon contamination, this can filter the cryostat volume in a few hours, allowing
 12 continuation of studies without having to refill. A schematic of the MTS is shown in
 13 Figure 1.2.
Fig:MIS Schem

14 The major conclusions of the studies to-date

15 today's to-date is different from when this was written

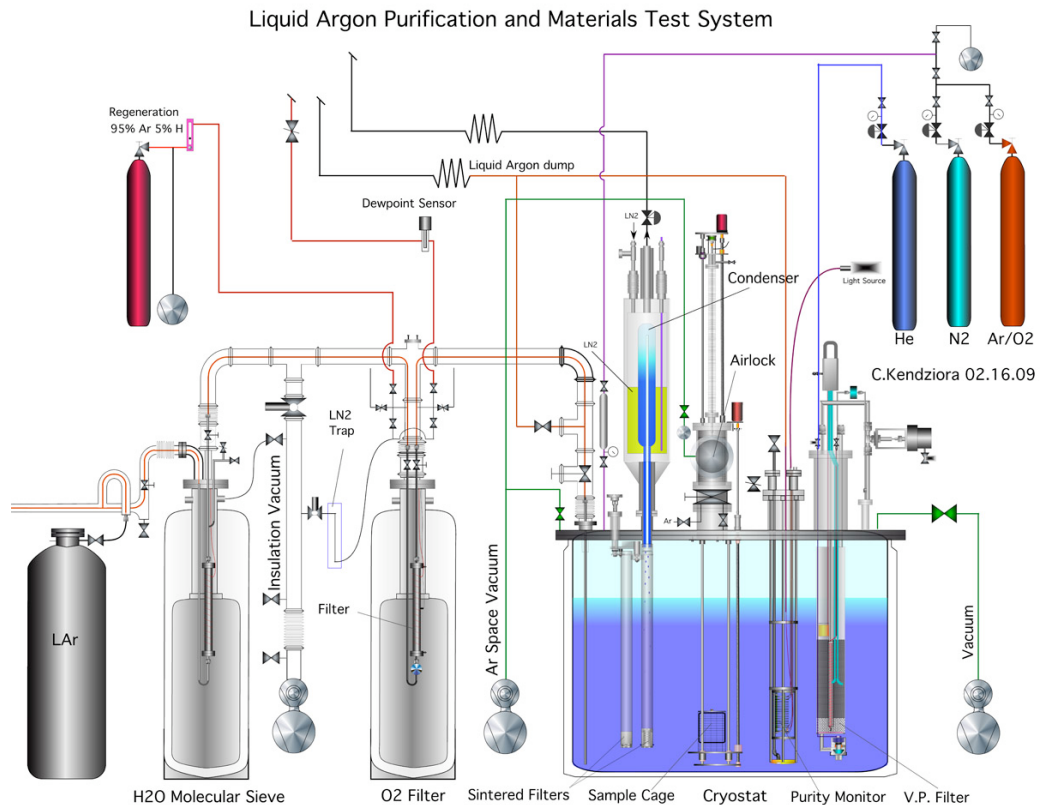


Figure 1.2: Schematic of the Materials Test System (MTS) cryostat at Fermilab

fig:MTS_Schem

Design for a Deep Underground Single-Phase LArTPC

1 are summarized here. No material has been found that affects the electron-drift
2 lifetime when the material is immersed in liquid argon – this includes, for example,
3 the common G-10 substitute, FR-4. On the other hand, materials in the ullage can
4 contaminate the liquid; this contamination is dominated by the water outgassed by
5 the materials and as a result is strongly temperature-dependent. Any convection
6 currents that transport water-laden argon into the LAr and any cold surfaces on
7 which water-laden argon can condense will fall into the LAr and reduce the electron
8 lifetime. Conversely, a steady flow of gaseous argon of a few ft/hr away from the
9 LAr prevents any material in the gas volume from contaminating the LAr.

10 These results are taken into account in the design of both MicroBooNE and LAr-
11 FD. For LBNE they have been cast as detector requirements. The MTS will continue
12 to be used by MicroBooNE and LBNE to test detector materials such as cables that
13 will reside in the ullage.

14 **1.4 TPC Design**

15 A string of recent events in several liquid argon setups, such as Long Bo, DarkSide50,
16 ArgonTube and MicroBooNE, in which the sustainable high voltage (HV) was much
17 lower than designed voltages

18 incomplete sentence

19 . These experiences prompted a reevaluation of the breakdown strength of liquid
20 argon, especially at “detector grade” purity. Recent studies [7][8] have revealed
21 that the HV-breakdown strength depends on factors such as electrode feature size,
22 distance, stress area/volume, and LAr purity. Although no conclusive threshold
23 was found, the results indicate that the safe operating field in LAr is well under
24 100 kV/cm.

25 With the uncertainty in the liquid argon HV dielectric strength, attention will
26 be focused on the HV-related aspects of the TPC design; this appears to involve the
27 CPAs and field cage modules.

28 right?

29 An R&D document has been compiled for the far detector

30 add citation

31 (docdb 10006) that contains a section on the proposed R&D topics and activities
32 to reduce the HV-related risks. Apart from the HV feedthrough, which will be
33 designed and tested above the operating voltages, there is a plan to improve the
34 designs of the CPAs and field cage modules.

1 The current TPC design directly interconnects all CPAs on a cathode plane.
2 Two of the outer cathode planes face the grounded cryostat walls. The stored energy
3 between one of the outer cathode planes and the cryostat wall, with the full bias
4 voltage applied, is more than 150 joules

5 add citation

6 (LBNE docdb 8920). This amount of energy, if released suddenly in an event of a
7 high voltage discharge, is sufficient to raise the temperature of a cube of stainless steel
8 with 2-mm sides by 4000°K, resulting in a leak in the membrane cryostat. Moreover,
9 a sudden collapse of the cathode voltage will also inject very large current pulses into
10 the front-end ASICs connected to the first induction plane wires, causing damage to
11 the electronics.

12 To minimize these risks, the logical steps are:

- 13 • minimize the stored energy when possible by swapping the locations of the
14 APA and CPA planes such that no CPAs are against the cryostat wall.
- 15 • slow the voltage collapse in a discharge by constructing the cathode planes out
16 of highly resistive material to form a long RC time constant for discharge
 - 17 – study the electrical behavior of CPAs constructed from highly resistive
18 material
 - 19 – identify and test a resistive coating that is robust at cryogenic temperature
20 and able to maintain good adhesion to the cathode structure
 - 21 – design the new CPAs with all resistive elements

22 Techniques for applying a highly resistive coating over the current 35t-style
23 printed circuit board-based panels on the field cage are being developed in order
24 to remove field concentration around the conductor edges. In parallel, a fall back
25 solution for reducing the field using roll-formed electrodes with a much larger edge
26 radius is being developed.

27 For the APAs, a simple and effective method to contain a broken outer layer wire
28 must be developed; such a wire must be prevented from drifting far into the drift
29 volume and making contact with the field cage.

30 1.5 35-ton Prototype: Phase 1

31 When first conceived, the 35-ton prototype cryostat was intended solely as a demon-
32 stration of membrane cryostat technology for use with liquid argon. Later, it was

35tonprototype

1 decided to install and operate a small-scale LArTPC in the cryostat to test many of
2 the design features proposed for use in the FD. The membrane cryostat demonstra-
3 tion, completed in 2014, is referred to as “Phase 1” and the operation of the TPC is
4 called “Phase 2.” Phase 2 is currently under construction and it is planned to take
5 data in summer 2015.

6 **1.5.1 Phase 1 Construction**

7 The construction of the 35t cryostat addressed a number of issues. First were
8 project-related issues, such as gaining detailed construction experience, developing
9 the procurement and contracting model, and incorporating the design and approval
10 mechanism in the Fermilab ES&H manual, which was necessary because membrane
11 cryostats are designed in accordance with European and Japanese standards. Sec-
12 ondly, it addressed technical issues such as high-purity operation in this type of
13 cryostat and the suitability of the planned LAr-FD construction techniques and ma-
14 terials.

15 The LBNE project contracted with the Japanese company IHI to build the 35t
16 cryostat at Fermilab. It was built in Fermilab’s PC-4 facility where the Liquid Argon
17 Purity Demonstrator (LAPD) [9] is also located, which allowed for re-use of a large
18 portion of the cryogenic-process equipment installed for LAPD. The proximity and
19 size (30 tons) of LAPD also offers the possibility using LAPD as a partial storage
20 vessel for LAr if the 35t ever needs to be emptied. The 35t employs a submersible
21 pump to pump the LAr from the cryostat to the filters. Two pumps were installed
22 for redundancy, but only one is used at a time. Figure 1.3 shows the layout of the
23 35t prototype at Fermilab’s PC-4 facility. Figure 1.4 shows a cutaway view of the
24 cryostat and a photograph of the interior of the completed cryostat.
tab:35tdimensions

25 Table 1.3 gives the details of the construction materials and the dimensions for
26 the 35t. More information can be found in [10]. The insulation thickness is 0.4 m
27 rather than the 1.0 m chosen for the reference design. The techniques of membrane-
28 cryostat construction were demonstrated to be a fit for high-purity TPC service.
29 Welding of corrugated panels, removal of leak-checking dye penetrant or ammonia-
30 activated leak-detecting paints, and post-construction-cleaning methods were tested
31 for suitability of service.
tab:membcryo1573

32 In principle, a thin-walled membrane cryostat is as suitable as a thick-walled
33 cryostat for use with high-purity LAr. Both are constructed with 304 stainless steel
34 with a polished surface finish. Both use passive insulation. The total length of
35 interior welds required for construction would be similar in both cases. The leak-
36 checking procedure would be the same in both cases.

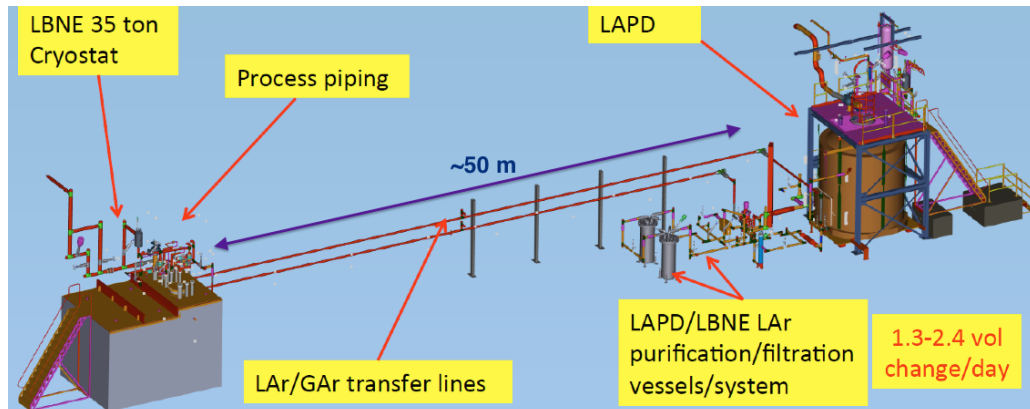


Figure 1.3: Layout of 35-ton prototype at Fermilab's PC-4 facility.

fig:35cryo

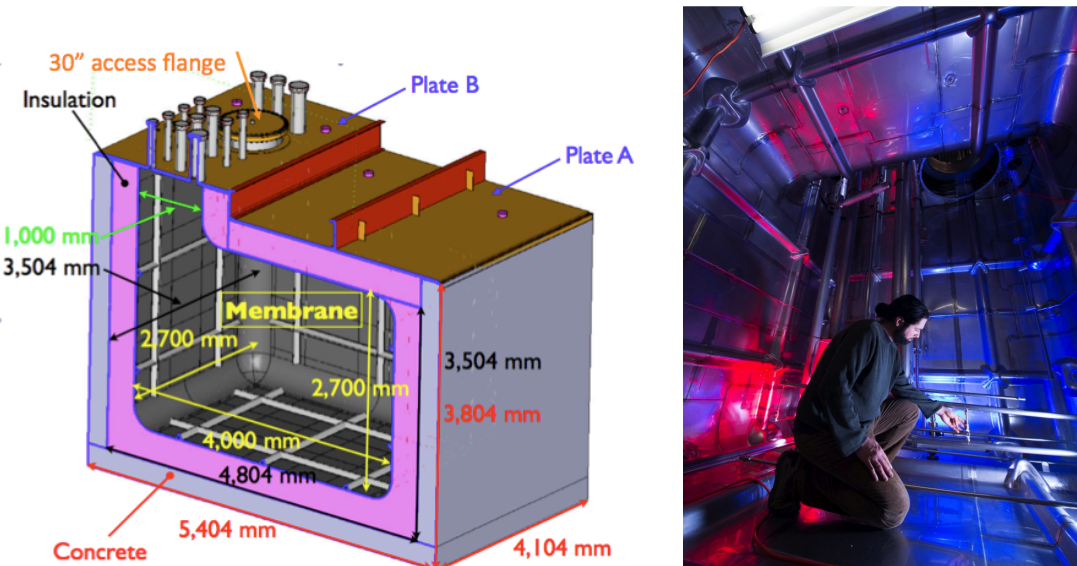


Figure 1.4: (left) Cutaway view of the 35t cryostat. (right) Interior photograph of the completed cryostat.

fig:35cutaway

Table 1.3: 35t Details and Dimensions

Parameter	Value
Cryostat Volume	29.16 m ³
Liquid Argon total mass	38.6 metric tons
Inner dimensions	4.0 m (L) x 2.7 m (W) x 2.7 m (H)
Outer dimensions	5.4 m (L) x 4.1 m (W) x 4.1 m (H)
Membrane	2.0 mm thick corrugated 304 SS
Insulation	0.4 m polyurethane foam
Secondary barrier system	0.1 mm thick fiberglass
Vapor barrier Normal	1.2 mm thick carbon steel
Steel reinforced concrete	0.3 m thick layer

:35Tdimensions

1 The significant difference between membrane cryostats and thick-walled cryostats
 2 is the depth of the welds used to construct the vessel. The majority of membrane-
 3 cryostat welds are completed in one or two passes with automatic welding machines.
 4 A second difference, and a major advantage, is that the membrane cryostat is a
 5 standard industrial design that has been in use for over 40 years. A thick-walled
 6 cryostat vessel would be custom designed and would require significant engineering
 7 and testing. A third difference, and another major advantage, is the ability to purge
 8 the membrane cryostat insulation space with argon gas so that a leak cannot affect
 9 the purity if it escapes detection and repair.

10 1.5.2 Phase 1 Instrumentation

11 The 35t includes a full complement of standard commercial transducers and sensors
 12 that are used to monitor and control the cryogenic environment. They include tem-
 13 perature sensors, pressure transducers (absolute and gauge), flow meters, and level
 14 sensors. These devices are typically read out directly into the Control System and
 15 data-logged.

16 A number of commercial gas analyzers are available

17 have been implemented?

18 that can measure trace impurity levels (O₂, H₂O, and N₂) in the argon. Some
 19 have sensitivities at the 100 ppt level. A gas distribution switchyard feeding the gas
 20 analyzers allows the sampling points in the 35t to be reconfigured.

21 There were also two purpose-built pieces of instrumentation for the monitoring of

the high-purity LAr environment, the purity monitors (PrMs) and the RTD Spooler.
The PrMs are used to measure electron lifetimes in the LAr, and the RTD Spooler is
used to make precision measurements of the temperature profile of the cryostat as a
function of depth. These instruments were originally constructed for the LAPD run
and are fully described in [9].

1.5.3 Phase 1 Operations

- In order to purify LAr, it is necessary to do three things:
1. Remove the air from the cryostat, leaving only Ar gas.
 2. Clean the liquid Ar as it comes from the supplier.
 3. Remove any impurities that are generated by materials outgassing within the cryostat.

LAPD has
executed all three of these processes and
demonstrated that it is not necessary to evacuate a cryostat in order achieve LAr purity levels sufficient for LBNE. This is of paramount importance since the costs of multi-kiloton cryostats that could withstand evacuation is prohibitive. The 35t followed the procedure LAPD [9] established to obtain and maintain pure LAr.

Gas Phase

Figure 1.5 graphically shows step 1 of the purification process, removal of the ambient air. These measurements are made by a variety of gas monitors that sample the gas in the cryostat.

When the test began, “dry” air had been purging the cryostat for approximately three weeks. The initial values for oxygen, water and nitrogen reflect this state. The Piston Purge removes the air in the cryostat; during this step argon gas is flooded into the bottom of the cryostat. Since argon is heavier than air, the argon layer rises, analogous to a mechanical piston, pushing the air up and out of the cryostat. This gas

the air?

is vented to the outside atmosphere. The venting stage continues for 32 hours, approximately the equivalent of 12 volume changes.

At this point the exiting gas

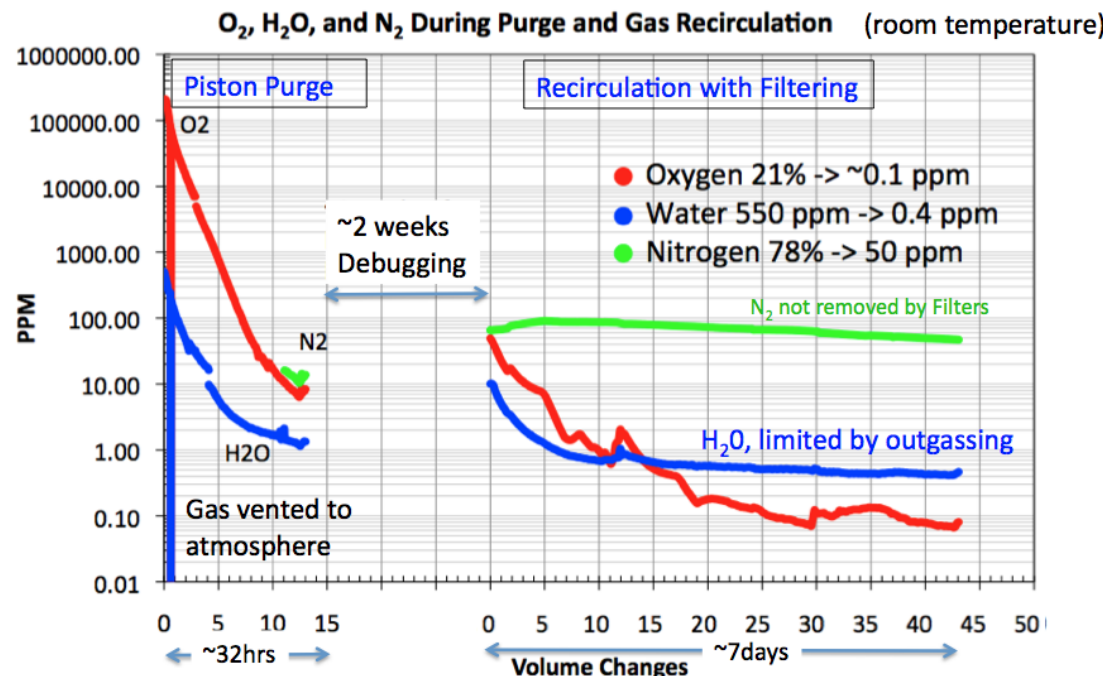


Figure 1.5: Gas phase of removing impurities in the 35t. These quantities are being measured by various gas analyzers. The first stage of the purification is a process called the “Piston Purge”. The second stage is “Recirculation with Filtering”. The gap between the two steps was due to troubleshooting a leak.

fig:35TPurge

which is mostly/all argon?

is re-routed to circulate through the filtration system that removes O₂ and H₂O.
(N₂ is not materially removed by the filters.) Any leaks to the outside atmosphere
can be detected during this step. As shown in Figure 1.5, a leak was found and
mitigated (the “Debugging” gap in the plot). Once leaks have been eliminated the
recirculation continues until the O₂ level drops to the sub-ppm level. As can be seen
in the plot, the H₂O level plateaus at a much higher level than O₂. This is due to
the outgassing of materials inside the 35t, including the cryostat walls, which are
remain?

at room temperature during
throughout?

the recirculation step.

Cooldown and LAr Fill

We have adopted a gas/liquid spray method to cool down the cryostat. This generates a turbulent mixing of cold gas in the cryostat and cools the entire surface. The cool down rate was limited to be less than the maximum rate specified by the membrane cryostat manufacturer. The cool down, as well as the initial filling is shown in Figure 1.6. The temperature measurements (red traces) in this plot were made by RTDs that are glued to the membrane walls of the cryostat. The black dashed trace is the manufacturer specification for the cool down rate.

Once the cool down was finished, the LAr transfer into the cryostat began. In the case of the 35t phase 1 run, the LAr came from LAPD, where it had been used by that system in its own recently completed second run[9].

LAPD contained about 30 tons of LAr, of which only 25 tons could be transferred to the 35t (~70% of the total possible 35t LAr volume). It was decided that we would begin the initial commissioning of the Phase 1 run with this level since several components of the 35 Ton could be commissioned with the partial LAr fill. After running with this partial fill for approximately eighteen days, additional LAr was added to bring the capacity to 100%.

LAr Purification

The Fermilab Material Test Stand (MTS)[11, 12] has shown that contaminants released inside LAr filled cryostats are from materials outgassing in the warm ullage

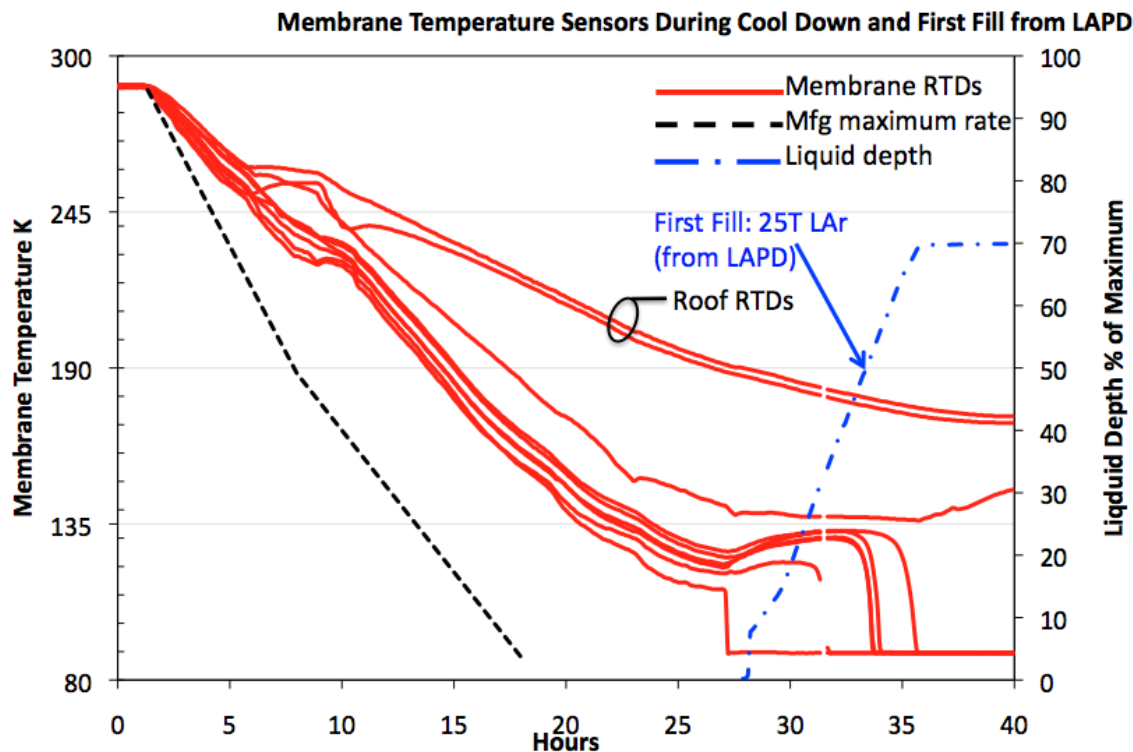


Figure 1.6: Cooldown and filling the 35t. The measurements (red trace) are made from RTDs afixed to the cryostat walls. The black dashed curve is the manufacturer's maximum allowed cooldown rate. The filling (blue trace) was from the transfer of LAr from LAPD, This quantity of LAr is less than the capacity of the 35t. The RTD traces drop to the LAr temperature when the level of the LAr covers reaches their mounting height.

fig:35TCooldown

21 regions above the LAr surface. Typical detector materials located in LAr have neg-
22 ligible impact of LAr purity levels.

23 Figure 1.7 depicts how impurities generated by outgassing materials in the rel-
24 atively warm ullage under Plate B are swept up by the normal Ar boil-off in the
25 35t. This impure vapor is condensed in the LN2-cooled LAr condenser. The im-
26 pure condensate is returned to the 35t just inside the intake manifold of the interior
27 submersible LAr pump. From there it is pumped to the filtration system where the
28 impurities are removed.

29 Of interest, the electron lifetime of the LAr exiting the filters, as measured by
30 the inline PrM was always > 30 ms (purity 10 ppt O₂ equivalent). This indicates
31 that the filters are very efficient at removing all trace amounts of O₂ and H₂O. This
32 was true for the entire 35t phase 1 run, including the filling periods.

33 Figure 1.8 shows the electron lifetime from the start of the LAr Pump operation
34 until the Phase 1 run ended. In general the electron lifetime improved as a function
35 of pump on-time, but there were several incidents that spoiled the lifetime. These
1 will be discussed in the next section.

2 1.5.4 Phase 1 Stability of Operation

3 The goals of the 35t Phase 1 run include not only achieving the required purity/lifetime
4 levels, but to also hold those levels and provide a stable operation of the cryostat.
5 The 35t Phase 1 run was a relatively short 2 months of LAr running. We achieved
6 electron lifetimes in the 2-3 ms range as can be seen in Figure 1.8.

7 However the electron lifetimes were severely impacted whenever we would switch
8 from one LAr pump to another. The drops in purity coincided with the turn on of
9 the previously-inactive pump (see annotations in Figure 1.8). We believe the issue
10 was with the procedure we used to start the pumps and plan to modify it for future
11 operations in the 35t Phase 2 run.

12 A second stability question is keeping the temperature stable in the cryostat. Cur-
13 rently the 35t controls system regulates the gauge pressure of the cryostat, keeping
14 the internal pressure to 6.69(02) kPa above ambient atmospheric pressure. However
15 this leaves the thermodynamics of the LAr sensitive to normal atmospheric pressure
16 changes.

17 Figure 1.9 is a plot over a nine day period of the Cryostat absolute pressure
1 (blue trace), bulk LAr temperature (white dashed trace) and the normalized drift
2 time of three PrMs, one short and long inside the cryostat, and the long inline
3 PrM exterior to the cryostat. The temperature is taken from the RTD Spooler
4 measurements by requiring that the RTDs be at least 15 cm below the LAr surface.

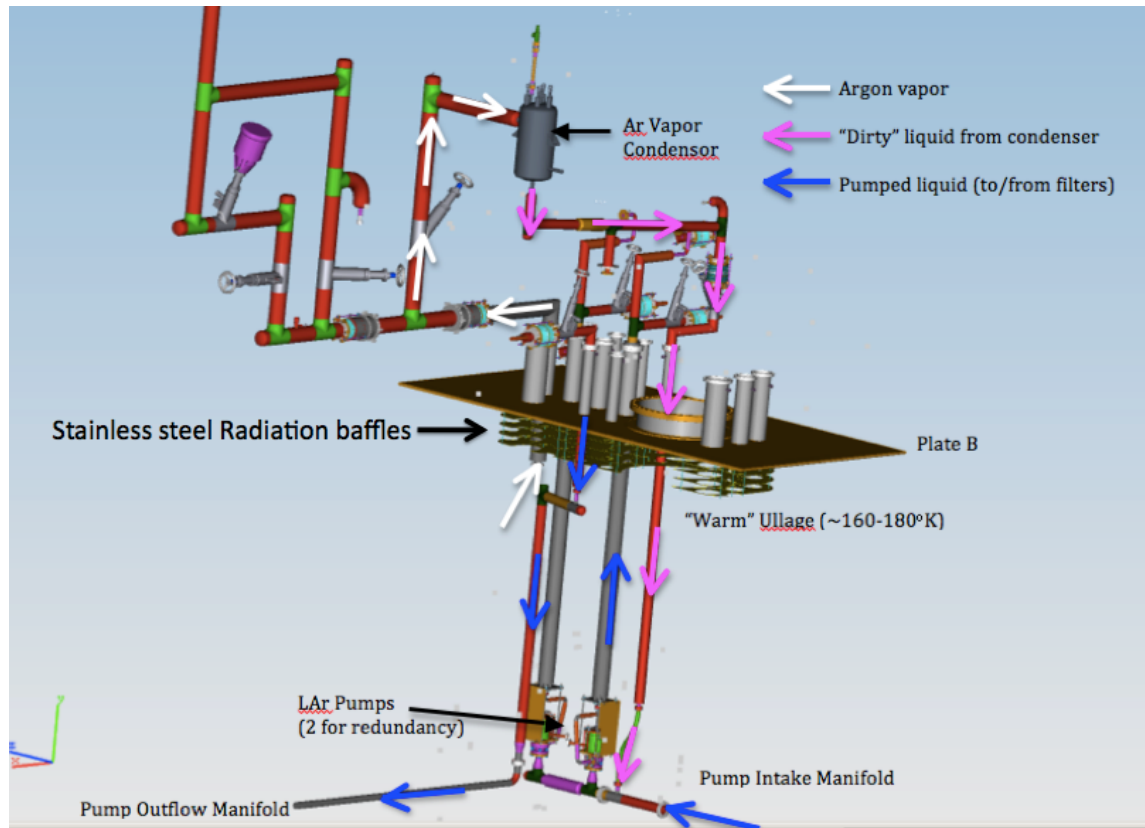


Figure 1.7: Drawing of Boiloff/Outgassing Vapor Flow (white arrows) from the 35t cryostat, with condensate return (violet arrows) from the condenser into the Pump Intake Manifold. LAr flow into the pump, and return from the Purification filters are shown by blue arrows. Also shown is the location of the Stainless Steel Radiation baffles beneath Plate B. This location just beneath Plate B is the warmest location and presumably the principal source of outgassing within the cryostat.

fig:35TVaporFl

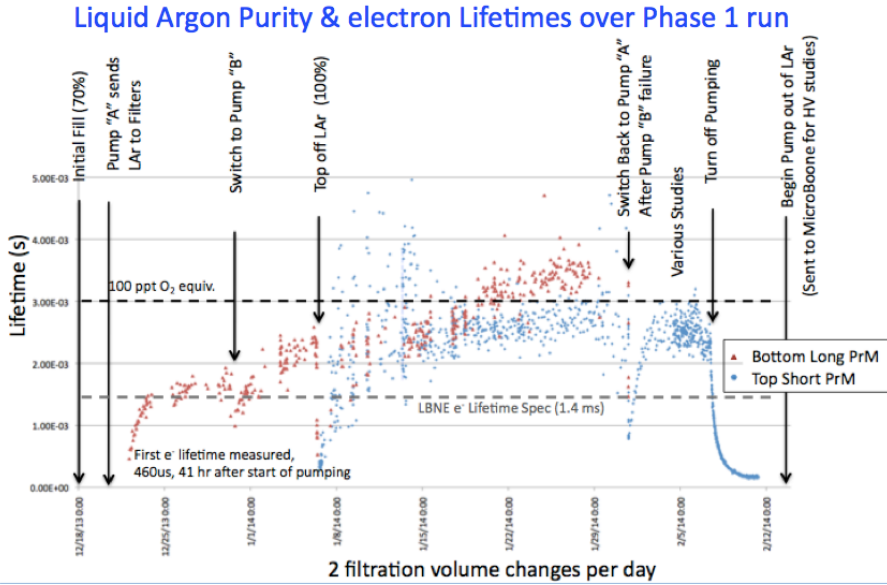


Figure 1.8: LAr electron lifetimes as measured by Cryostat Purity Monitors. Significant events are annotated on the plot. Major divisions on horizontal axis are one week periods. Equivalent purity levels are shown as dashed horizontal lines.

fig:35TElectro

- 5 The temperature curve lags the pressure changes ($\Delta P \sim 3.5$ kPa over this period),
 6 due to the thermal inertial of the LAr. However the normalized drift time (= drift
 7 time/(average drift time for this period) is directly correlated to the LAr temperature.
 8 The LAr temperature excursion range was $\Delta T \sim 0.3$ K. Fitting the normalized drift
 9 velocity (inverse of normalized drift time) gives the result

10 $\Delta_{driftspeed/\overline{driftspeed}} = -0.022/001\text{ K}$

11

- 12 The electron drift velocities for these three PrMs varied from (0.3 to 0.4) mm/ μ s
 13 depending on the individual PrM's drift field.

- 14 The RTD Spooler was intended to give us a precision measurement of the vertical
 15 temperature profile. This measurement is a means of testing the Computational
 16 Fluid Dynamics Simulations [5]

17

- 1 that are being made on the fluid motion in the cryostat. Experimentally mea-
 2 suring the actual motion does not appear to be feasible at this time. The CFD
 3 calculations are being used to understand whether there might be dead areas in the
 4 cryostat where impurities might collect. Figure 1.10 shows the result of one RTD
 5 scan. This scan was taken from a period where the barometric pressure was relatively

fig:SpoolerScan

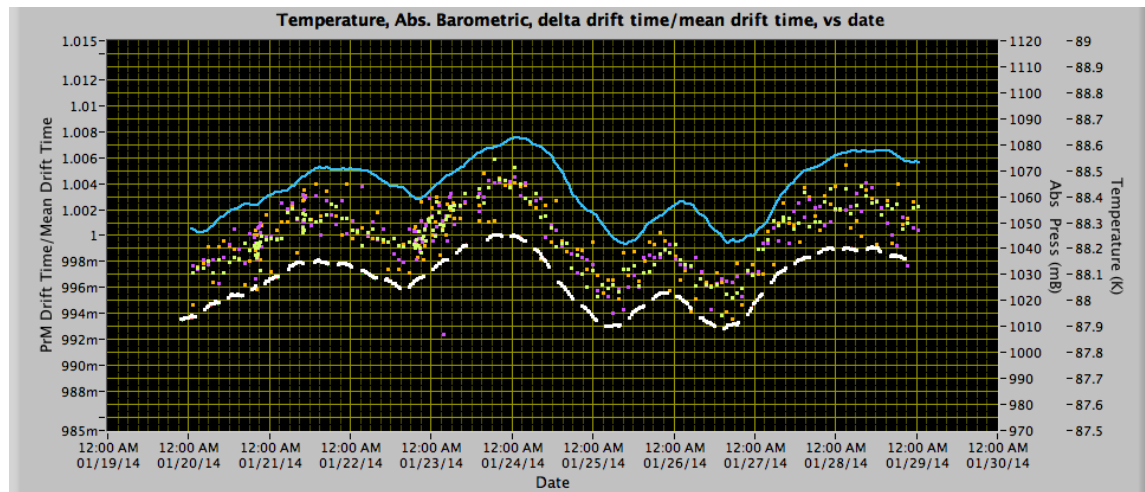


Figure 1.9: Interior Cryostat Absolute Pressure (blue trace), bulk LAr temperature (white dashed trace), and PrM drift times (dots) over a nine-day period. Major divisions on horizontal axis are one day intervals. The PrM drift times are from three PrMs, two in the cryostat, and the third from the inline PrM. The lag between the temperature and pressure is due to the 35t thermal inertia.

fig:35TTempSta

constant so that the temperature would remain constant during the scan. Since a scan takes up to 6 hours in one direction (up or down) and as can be seen in Figure 1.9, pressure changes can impact the bulk temperature of the LAr. These profiles seen in Figure 1.10 are in nominal agreement with the current CFD calculations [5].

1.5.5 Phase 1 Conclusions

The 35t Phase 1 run has shown that the membrane cryostat technology has no innate difficulties with achieving the stated goals of the LBNE Conceptual Design Far Detector. Some of the 35t issues (e.g., loss of purity when pumps are switched) are most likely unique to the 35t. It also seems likely that in a future design, the pumps will be externally located, to avoid coupling acoustical vibrations into the Far Detector cryostat and to facilitate maintenance and repair.

1.6 35t Prototype Phase 2

Phase 2 of the the 35t prototype involves installing a fully operational TPC and Photon Detector into the previously built cryostat. This prototype will be filled with Liquid Argon and operated for a several-month-long Cosmic Ray run. External plastic scintillator paddles placed around the cryostat will be used to produce trigger signals as well as rough position measurements of the incoming Cosmic Rays. Installation of the TPC inot the cryostat is expected in April 2015 and commissioning is expected to begin in June 2015. Figure 1.11 shows a model of the TPC inside the cryostat and a trial assembly of the TPC done outside of the cyrostat.

1.6.1 35t Phase 2 TPC Design

The Phase 2 prototype incorporates many of the design elements described in previous sections of this document. In many cases, these include novel features that have never previously been tested in an operational TPC. Rather than reiterate them all here, we simply tabulate some of the more important aspects in Table 1.4.

1.6.2 Phase 2 Simulation, Reconstruction and Analysis

As can be seen from Table 1.4, successful tests of many of the new design features requires simulation, reconstruction and analysis of 35t data. This will be done with

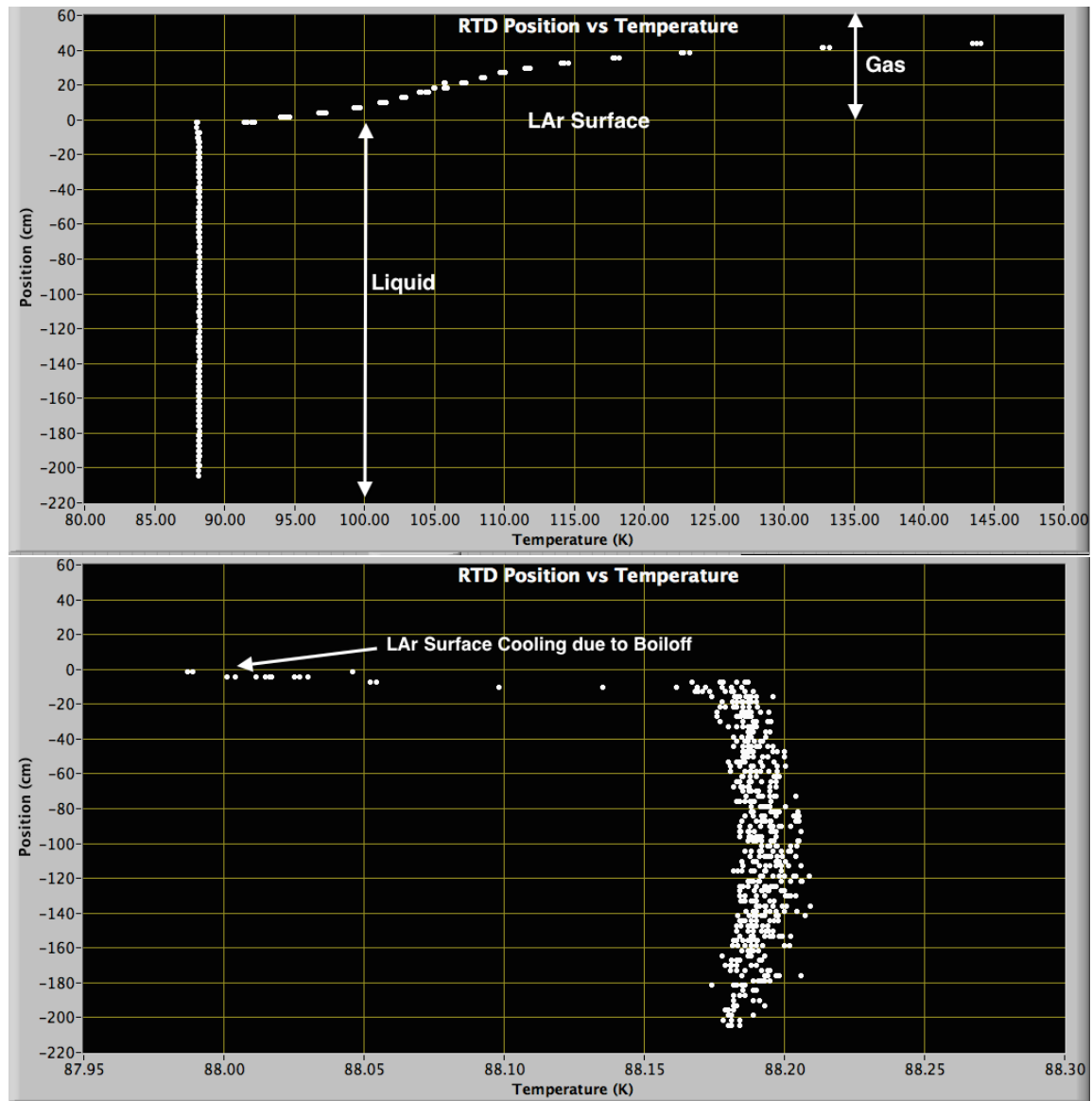


Figure 1.10: (top) RTD Spooler Vertical Temperature scan of the 35t Cryostat under Plate B showing both the liquid and vapor temperature. (bottom) Expanded horizontal axis around 88.12 K. Note that the horizontal divisions on the lower plot are 50 mK.

fig:SpoolerScan

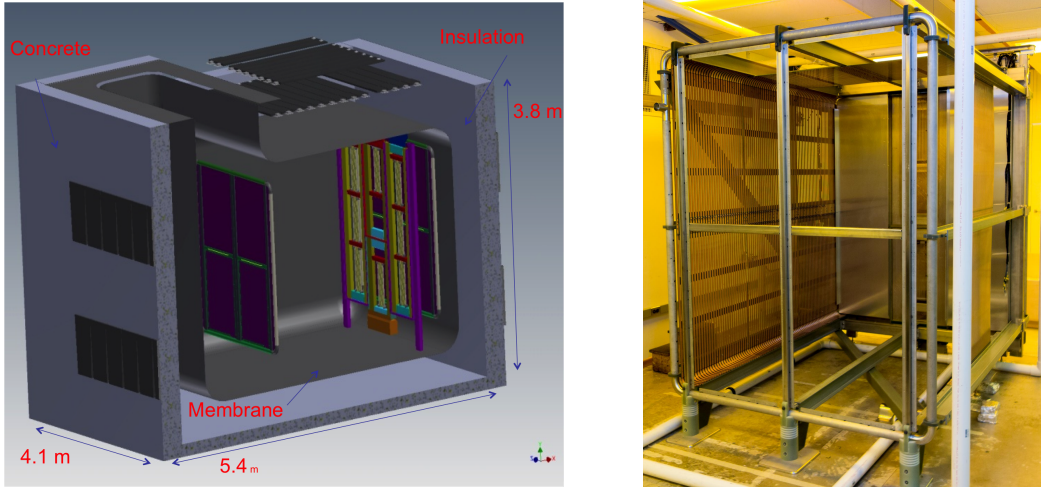


Figure 1.11: (left) 35t Cryostat with TPC and photon detectors installed. Note separate drift regions on “near” and “far” sides. The near side drift length is close to what is proposed for the far detector. The far side has a shorter drift length due to lack of space. (right) A trial assembly of the TPC.

fig:35TPC

Table 1.4: 35t Design Elements

Design Aspect	Section	How Tested
Modular APAs with wrapped wires	?? <small>subsec:vb_tpc_chamber_apas</small>	Build small-scale APA Modules with FD design
Vertical Gaps between APAs	?? <small>subsec:vb_tpc_chamber_apas</small>	Assemble APAs side-by-side. Study reco'd tracks that cross the gaps.
Horizontal Gaps between APAs	?? <small>subsec:vb_tpc_chamber_apas</small>	Build two shorter APAs and stack vertically Study reco'd tracks that cross the gaps
APAs immersed in active volume	?? <small>subsec:vb_tpc_chamber_apas</small>	Study reco'd tracks that cross APAs
Cold Digital Electronics	?? <small>subsec:fo_CMOS_digital</small>	Measure noise performance etc. <i>in situ</i>
Waveguide-style Photon Detector	?? <small>sec_daq_intro</small>	Install in APAs. Measure lightyield
Triggerless-capable DAQ	??	Take data using multiple DAQ modes

tab:35TDesign

7 the help of the LarSoft package, which is also used to simulate and reconstruct
8 data from the ArgoNeuT and MicroBoone experiments. Reuse of software developed
9 for those experiments can greatly facilitate 35t development. However, the novel
10 hardware features of the 35t prototype necessitate novel software developments as
11 well. Among the required new software developments are:

- 12 ● Code to break up the wrapped wires into as many as five individual linear
13 segments. A hit on a single electronic channel can, in principle, be related to
14 an induced signal on any of these segments.
- 15 ● “Disambiguation” code to identify which of the possible wire segments was
16 actually responsible for the observed hit
- 17 ● Code for determining the start time of the event (t_0). Since the 35t prototype
18 DAQ can run “triggerless”, methods are needed for finding the t_0 in data.
19 Information from the external scintillator paddles as well as the internal photon
20 detectors can be used.
- 21 ● Code for “stitching”together track segments observed in different tracking vol-
22 umes. Since hits can come from either side of the 4 APAs, there are effectively
23 8 separate tracking volumes, which are treated as separate TPCs.

24 With these simulation and reconstruction tools in hand, “physics” analysis of
25 the data can be undertaken. In addition to the analyses needed to validate the new
26 detector design elements, there are also some analyses of basic LArTPC performance
27 that are needed as well. Among the highest priority analysis tasks are:

- 28 ● Basic detector performance: signal/noise, purity measured with tracks, track
29 direction resolution, photon detector light yield
- 1 ● Measurement of distortions due to space charge and field non-uniformity
- 2 ● Measurements of different types of particles: muons, protons, neutrons, pions

3 The results obtained by operating the 35t Phase 2 prototype and the analysis of
4 its data are expected to be very valuable in defining the final FD design.

5 **1.7 Prototype Detector at CERN to Test Physics Sen- 6 sitivity**

7 The physics sensitivity of DUNE has been estimated based on detector-performance
8 characteristics published in the literature, simulation-based estimates and on a vari-
9 ety of assumptions about the anticipated performance of the future detector, event
10 reconstruction and particle-identification algorithms. A single-phase LAr prototype
11 detector has been proposed for testing in a CERN beam with the goal of replacing
12 these assumptions with measurements. The prototype will implement a full-scale de-
13 tector element; this will mitigate the risks associated with extrapolating from small-
14 scale versions of the single-phase LAr TPC technology and allow benchmarking of
15 the operation of a full-scale detector elements in a well characterized charged-particle
16 beam.

17 The detector will need to accurately identify and measure the energy of the particles produced in the neutrino interaction with argon, which will range from hundreds of MeV to several GeV. The beam measurements will serve as a calibration data set to tune the Monte Carlo simulations and serve as a reference data set for the detector.

22 The prototype is expected to identify any potentially problematic components and lead to future improvements and optimizations of the detector design.

24 **1.8 Physics Experiments with Associated Detector- 25 Development Goals**

26 Two projects, ArgoNeuT and MicroBooNE, which are physics experiments in their own right, are also contributing to the development of the LBNE experiment. Their most important role is in providing data and motivation for the development of event reconstruction and identification software.

30 **1.8.1 ArgoNeuT - T962**

31 The Argon Neutrino Test (ArgoNeuT) is a 175-liter LArTPC which completed a run in the NuMI neutrino beam. The $0.5\text{ m} \times 0.5\text{ m} \times 1\text{ m}$ LArTPC was positioned directly upstream of the MINOS near detector, which served as a muon catcher for neutrino interactions occurring in ArgoNeuT.

2 ArgoNeuT began collecting data using the NuMI anti-muon neutrino beam in
3 October 2009 and ran until March 1, 2010. ArgoNeuT's $\sim 10\text{k}$ events motivate the

development of analysis tools, and are the basis for the first measurements of neutrino cross sections on argon. An event with two π^0 decays is shown in Figure 1.12. ArgoNeuT was also the first LArTPC to be exposed to a low-energy neutrino beam and only the second worldwide to observe beam-neutrino interactions. The ArgoNeuT collaboration is currently preparing (1) a NIM paper that documents the detector performance using NuMI beam muons and (2) the first physics paper on muon-neutrino charged-current differential cross sections on argon. See Figures 1.14 and 1.15.

A deconvolution scheme using an FFT has been applied to the ArgoNeuT data. This procedure eliminates a problem with the ArgoNeuT electronics (which were D-Zero spares and could not be modified for ArgoNeuT). Another more significant benefit of deconvolution is that bi-polar induction-plane signals can be transformed into uni-polar collection-plane signals. An example of this is shown in Figure 1.13. A selection of figures from the draft NIM paper are reproduced below.

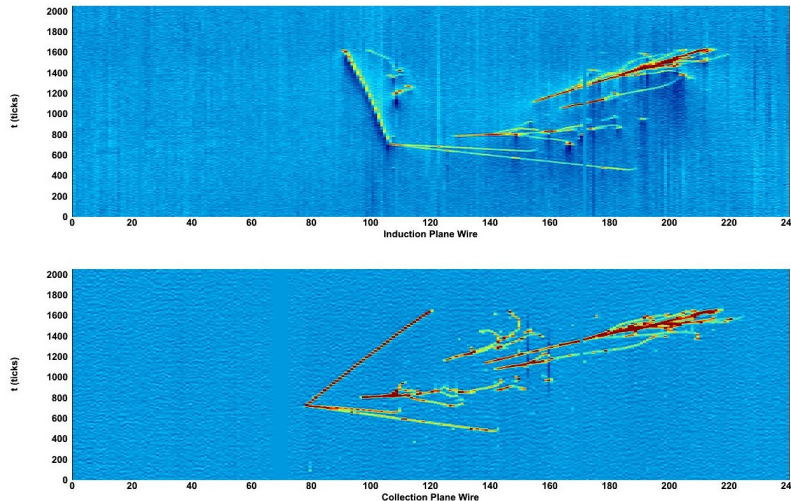


Figure 1.12: A neutrino event with four photon conversions in the ArgoNeuT detector. The top (bottom) panel shows data from the induction (collection) plane after deconvolution.

The applicability of ArgoNeuT is that it provides a set of data in the same range of energy as the LBNE neutrino beam, enabling the development of analysis algorithms that can be utilized for LAr-FD physics analysis with little or no modification.

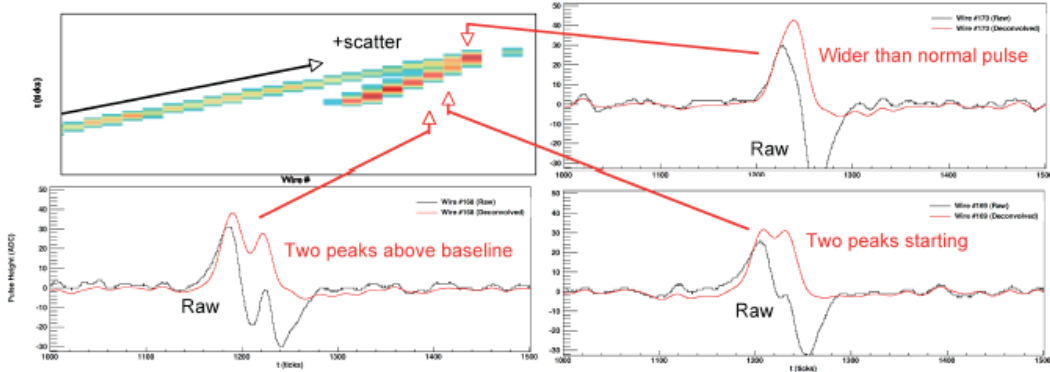


Figure 3: (Upper left) A set of tracks as seen on the (deconvoluted) induction plane. The wire views on three adjacent wires are also shown in order to demonstrate the effects of deconvolution on the raw wire pulses. The raw data can be seen in black and the deconvoluted data can be seen in red.

Figure 1.13: Figure from the ArgoNeuT draft NIM paper

fig:Argo-decon

1.8.2 MicroBooNE E-974

The MicroBooNE experiment is an 89-ton active mass LArTPC, (170-ton argon mass) in the commissioning phase. It has both a physics program and LArTPC development goals.

MicroBooNE received stage 1 approval from the Fermilab director in 2008, partial funding through an NSF MRI in 2008 and an NSF proposal in 2009. MicroBooNE received DOE CD-0 Mission Need in 2009, CD-1 review in 2010, CD-2/3a review in 2011, CD-3b review in 2012 and CD-4 review in December 2014. The construction of MicroBooNE experiment has been completed successfully, and detector commissioning is ongoing. It plans to start running in mid 2015.

As well as pursuing its own physics program, MicroBooNE will collect a large sample ($\sim 100k$) of low-energy neutrino events that will serve as a library for the understanding of neutrino interactions in LAr. Because MicroBooNE is at the surface, it will also have a large sample of cosmic rays with which it can study potential backgrounds to rare physics. The process of designing MicroBooNE has naturally stimulated several developments helpful to the LBNE program. Studies of wire material, comparing Be-Cu with gold-plated stainless steel in terms of their electrical and mechanical properties at room and LAr temperatures, and techniques for wire-tension measurement are immediately relevant. Expertise has been developed gen-

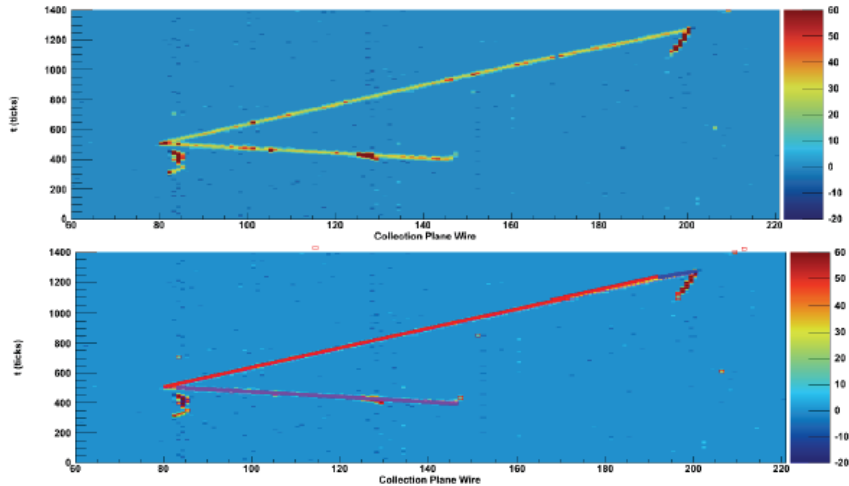


Figure 6: (Top) A neutrino candidate in ArgoNeuT as seen on the collection plane. (Bottom) The Hough lines found with the line-finding algorithm overlaid on the particle tracks.

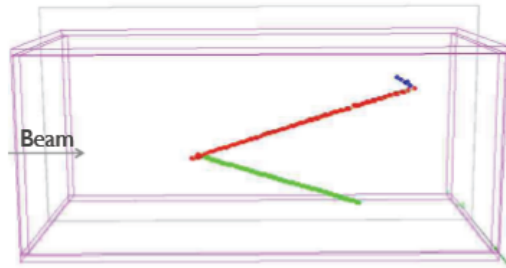


Figure 7: The neutrino event shown in Figure 6 reconstructed in three dimensions.

Figure 1.14: Figure from the ArgoNeuT draft NIM paper showing the status of 3D reconstruction

fig:ArgoNeuT_3

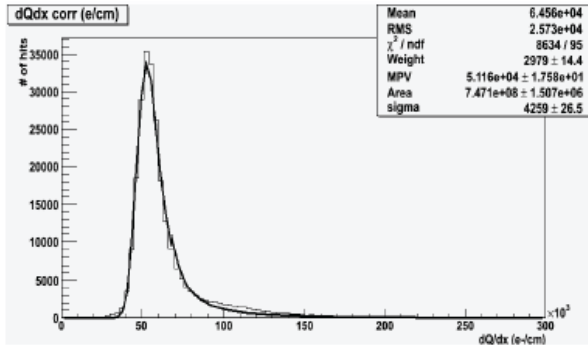


Figure 13: dQ_0/dx distribution (in ADC/cm) obtained for the through-going muon data sample having corrected for the electron lifetime and quenching effect on the ionization charge and properly taken into account the contribution due to δ -rays, as reported in the previous Section. A Landau-Gaussian fit is also reported.

Figure 1.15: Figure from the ArgoNeuT draft NIM paper showing the status of calorimetric reconstruction.

fig:ArgoNeuT-

erating simulations of electrostatic-drift fields as well as simulations of temperature and flow distributions in LAr cryostats which is being applied to the LAr-FD TPC and cryostat. MicroBooNE will use the front end of the proposed in-liquid electronics as the wire-signal amplifiers and the DAQ developed for MicroBooNE will exploit compression and data-reduction techniques to record data with 100% livetime. In summary, MicroBooNE's LArTPC development goals that are pertinent to LAr-FD are

- large-scale testing of LBNE cryogenic front-end electronics, similar in scale to the CERN prototype
- testing of continuous data-acquisition algorithms
- refinement of the analysis tools developed in ArgoNeuT
- provide costing and construction lessons-learned

1.9 Summary

Impressive progress has been made in the development of LArTPC technology over the last few years. All elements of the development program have completed the

¹ R&D phase. Credible conceptual designs exist for all systems in LAr-FD. The technical activities described in this chapter are properly characterized as preliminary engineering design.

⁴ The most significant deficiency is the lack of fully-automated event reconstruction. Algorithms have been developed within the LAr community and are being successfully applied to ArgoNeuT data as well as to simulated MicroBooNE data. ⁶ The algorithms have individually shown that the high efficiency and excellent background rejection capabilities of an LArTPC are achievable. The task remains to ⁷ combine them into a single package. ⁸

¹⁰ Bibliography

- ¹¹ [1] A. Himmel, “Transmission vs. angle.” LBNE DocDB 7599-v2, 2013.
- ¹² [2] V. Gehman *et al.*, “Fluorescence efficiency and visible re-emission spectrum of
¹³ tetraphenyl butadiene films at extreme ultraviolet wavelengths,” *Nucl. Instrum.
Meth. A*, vol. 654, p. 116, 2011.
- ¹⁵ [3] L. Bugel *et al.*, “Demonstration of a lightguide detector for liquid argon TPCs,”
¹⁶ *Nucl. Instrum. & Meth.*, vol. A640, p. 69, 2011.
- ¹⁷ [4] B. Baptista and S. Mufson, “Comparison of TPB and bis-MSB as VUV
¹⁸ waveshifters in prototype LBNE photon detector paddles,” *JINST*, vol. 8,
¹⁹ p. C09006, 2013.
- ²⁰ [5] S. Mufson and B. Baptista, “Light guide production for LBNE and the effects
²¹ of UV exposure on VUV waveshifter efficiency,” *JINST*, vol. 8, p. C09012, 2013.
- ²² [6] B. Baller, B. Fleming, “Integrated Plan for LArTPC Neutrino Detectors in the
²³ US,” tech. rep., FNAL, 2010. LBNE:DocDB-2113.
- ²⁴ [7] A. Blatter *et al.*, “Experimental study of electric breakdowns in liquid argon at
¹ centimeter scale.” arXiv:1401.6693.
- ² [8] B. Acciarri *et al.*, “Liquid argon dielectric breakdown studies with the micro-
³ boone purification system.” arXiv:1408.0264.
- ⁵³⁸ [9] M. Adamowski *et al.*, “The liquid argon purity demonstrator,” *JINST*, vol. 9,
⁵³⁹ p. P07005, July 2014.
- ⁵⁴⁰ [10] Cryogenic Engineering Conference: Advances in Cryogenic Engineering, *First
541 Scientific Application of the Membrane Cryostat Technology*, 2014.
- ⁵⁴² [11] E. Voiron *et al.*, “35 ton cryostat liquid argon flow, temperature, and charge
⁵⁴³ density cfd simulation.” LBNE DocDB 9940-v1, November 2014.

- 544 [12] B. Rebel *et al.*, “Results from the fermilab material test stand and status of
545 the liquid argon purity demonstrator,” *Journal of Physics: Conference Series*,
546 vol. 308, 2011.